A refined human linear B cell epitope map of Outer surface protein C (OspC) from the Lyme disease spirochete, *Borreliella burgdorferi*

Grace Freeman-Gallant[1,#], Kathleen McCarthy[2, #], Jennifer Yates[1,2], Karen Kulas[1], Michael J. Rudolph[3], David J Vance[1,2], and Nicholas J Mantis[1,2,*]

[1] Division of Infectious Diseases, Wadsworth Center, New York State Department of Health, Albany, NY; [2] Department of Biomedical Sciences, University at Albany, Albany, NY;[3] New York Structural Biology Center, New York, NY

[#], these authors contributed equally to this study with last names listed alphabetically

Running title: Linear B cell epitopes on OspC

*, address correspondence to Dr. Nicholas Mantis, Division of Infectious Diseases, Wadsworth Center, New York State Dept Health, 120 New Scotland Ave, Albany, NY 12208; Tel: 518-473-7487; Email:nicholas.mantis@health.ny.gov

ABSTRACT

A detailed understanding of the human antibody response to Outer surface protein C (OspC) of *Borrelellia burgdorferi* has important implications for Lyme disease diagnostics and vaccines. In this report, a total of 13 peptides encompassing eight reported OspC linear B cell epitopes from OspC types A, B and K, including the conserved C-terminus (residues 193-210: peptide C10), were evaluated by multiplex immunoassay (MIA) for IgG reactivity with ~700 human serum samples confirmed positive in a two-tiered Lyme disease diagnostic assay and ~160 post-treatment Lyme disease (PTLD) serum samples. The VlsE C6-17 peptide was included as a positive control. Diagnostic serum IgG reacted with 11 of the 13 OspC-derived peptides, significantly more than controls, with the C10 peptide being the most reactive. In the PTLD serum samples, two OspC peptides including C10 were significantly more reactive than controls. Spearman's rank correlation matrices and hierarchical clustering indicated a strong correlation between C10 and VlsE C6-17 peptide reactivity but little demonstrable association between C10 and the other OspC peptides or recombinant OspC. OspC peptide reactivities (excluding C10) were strongly correlated with each other and were disproportionately influenced by a subset of pan-reactive samples. In the PTLD cohort, C10 clustered with the other OspC-derived peptides and was distinct from OspC and VlsE C6-17. The asynchronous serologic response to OspC, C10, and the OspC-derived peptides reveals the complexity of B cell responses to *B. burgdorferi* and confounds simple interpretation of antibody profiles associated with Lyme disease.

IMPORTANCE

Lyme disease is an emerging tick-borne infection caused by the spirochete, *Borreliella burgdorferi*. In humans, antibodies against spirochetal outer surface lipoproteins are proposed to play a role in disease resolution and in protection against reinfection. Some of those same antibodies also serve as diagnostic indicators of an active or history of Lyme disease. In this study, we sought to validate reported antibody binding sites on Outer surface protein C (OspC), a known target of both protective and diagnostic antibodies.

KEYWORDS: Lyme disease, antibody, epitope, vaccine, *Borrelia burgdorferi*

56 **INTRODUCTION**

57 Lyme (borreliosis) disease is the most common vector-borne infection in the United
58 States, with an estimated 450,000 cases per year (1). The primary etiologic agent of Lyme
59 disease is the spirochetal bacterium, *Borreliella burgdorferi*. In North America, the spirochete is
60 transmitted to humans by black legged ticks, *Ixodes scapularis* and *Ixodes pacificus*, during the
61 course of a blood meal. The spirochete proliferates at the site of the tick bite, typically resulting
62 in an expanding skin lesion commonly referred to as a bull's eye rash or erythema migrans (2-4).
63 In the absence of antibiotic intervention, *B. burgdorferi* can disseminate to peripheral tissues,
64 organs, large joints, and the central nervous system, potentially resulting in severe complications
65 including neuroborreliosis, carditis and/or Lyme arthritis weeks, months or even years later (2,
66 5). Moreover, a fraction of Lyme disease patients who receive a full regimen of antibiotics will
67 report persistent health issues (e.g., fatigue, cognitive issues, musculoskeletal pain), a syndrome
68 termed post-treatment Lyme disease (PTLD) (6-9). Developing rapid and accurate diagnostic
69 tests capable of detecting and discriminating between LD, PTLD syndrome and *B. burgdorferi*
70 reinfection are much needed (2l, 10).

71 The humoral response to *B. burgdorferi* is robust, resulting in detectable spirochete-
72 specific B cells and serum IgM and IgG days and weeks following an infectious tick bite (11-
73 14). In Lyme disease patients, antibodies are primarily directed against *B. burgdorferi*'s panoply
74 of outer surface lipoproteins (15). Among these, Outer surface protein C (OspC; also known as
75 BB_B19, P23 and P25) stands out. OspC is a ~21 kDa helical homodimeric lipoprotein
76 expressed by *B. burgdorferi* during tick transmission and in the early stages of infection (16).
77 OspC is implicated in facilitating spirochete egress from the tick during the course of a blood
78 meal, enabling survival in the early stages of mammalian skin infection, and modulating
79 transmigration across vascular walls (16-23). The highly immunogenic nature of OspC has lent
80 itself to applications in Lyme disease serology-based diagnostics, including widely used
81 commercial tests (24, 25). For example, the peptide derived from the conserved C-terminal 10
82 amino acids of OspC (peptide "C10") is a component of the FDA approved diagnostic test
83 *Borrelia* VlsE1/pepC10 from Zeus Scientific (Branchburg, NJ) (26-30). In addition to their
84 diagnostic utility, linear B cell epitopes from different OspC types are a component of a widely
85 used canine Lyme disease vaccine and being considered for human use (see references within
86 (31)).

87 While multiple linear human B cell epitopes on OspC have been reported over the past
88 three decades, differences in serologic assays, detection methodologies, and sample sizes from
89 varying Lyme disease cohorts, makes it difficult to draw conclusions about relative reactivities of
90 one peptide over another. This is problematic, because determining the relationships between
91 OspC-derived peptides (including C10) and total OspC antibodies has practical implications for
92 interpreting serologic assays. Moreover, there are >26 allelic variants or types of OspC reported
93 in the United States, with amino acid sequence identities that range from 60-90% (32, 33). As
94 different OspC types are associated with varying degrees of virulence and invasiveness, tracking
95 epitope-specific responses to those particular types is of paramount importance (34, 35). In New
96 York state, for example, OspC types A, B and K, which are associated with more invasive
97 disease, represent ~70% of all isolates (35-37).
98 With that in mind, we sought to validate human antibody reactivities to reported linear epitopes
99 associated with OspC to enable broad comparability of epitope usage across *B. burgdorferi* for
100 diagnostic and vaccine development purposes.
101
102 **METHODS**
103
104 **Chemicals and biological reagents**. Chemicals and reagents were obtained from Thermo Fisher
105 Scientific (Waltham, MA), unless noted otherwise. Buffers were prepared by the Wadsworth
106 Center's Cell and Tissue Culture core facility.
107
108 **Recombinant OspC and OspC-derived peptides.** Recombinant *B. burgdorferi* $OspC_A$
109 (residues 38 to 201; PDB ID 1GGQ; UniProt ID Q07337) (38), $OspC_B$ (residues 38 to 202; *B.*
110 *burgdorferi* strain ZS7; PDB ID 7UJ2) (39) and $OspC_K$ (residues 38 to 202; *B. burgdorferi* strain
111 297; PDB ID 7UJ6) (40) were expressed in *E. coli* strain BL21 (DE3) and purified by nickel-
112 affinity and size-exclusion chromatography, as described (41). Recombinant $OspC_A$ with the C10
113 sequence (residues 201-210; PVVAESPKKP; "$OspC_A$+C10") was expressed and purified as
114 above. Linear epitope prediction was done using Discotope 2.0 (42). OspC peptides (>80%
115 purity) were synthesized by Genemed Synthesis (San Antonio, TX) with a C-terminal GGGSK-
116 biotin extension. We also synthesized the VlsE-derived C6 B31-17 peptide
117 [MKKDDQIAAAIALRGMA] with the GGGSK-biotin linker (43).

118

119 **Commercial and clinical LD serum samples.** Commercial Lyme disease seronegative (Lot
120 10500586) and seropositive (Lot 10510438) pooled samples were used strictly as intra-assay and
121 bead coupling confirmation controls throughout this study (ACCURUN products 810 and 130,
122 respectively; SeraCare, Milford, MA). The Lyme disease seronegative samples (referred to as
123 "controls" throughout the manuscript) consist of a commercial panel of 81 serum samples
124 collected in 2017-2018 (Access Biologicals, Vista, CA). Five of the 81 serum samples were
125 classified as extreme outliers for VlsE C6-17 reactivity by interquartile range (IQR) calculated
126 using Microsoft Excel and therefore removed from the control panel. In the end, a total of 76
127 control samples were used as comparators with the diagnostic sample set and 75 samples were
128 used as comparators for the PTLD sample set as a result of sample availability.
129 *B. burgdorferi* seropositive serum samples (n = 696) were obtained from the New York
130 State Department of Health Wadsworth Center's Diagnostic Immunology Laboratory. The
131 samples had been submitted for Lyme disease serology and subjected to two-tiered testing
132 consisting of (Tier 1) a C6 peptide screen (Immunetics®; C6 Lyme ELISA™) or Enzyme
133 Linked Fluorescent Assay (ELFA; BioMerieux, VIDAS® Lyme IgG II and Lyme IgM II;
134 Durham, NC), followed by (Tier 2) IgM and IgG detection by Western blot (MarDX®; Trinity
135 Biotech, Carlsbad, CA). *B. burgdorferi*-specific IgM reactivity was defined as ≥2 positive bands,
136 with IgG reactivity defined as ≥5 positive bands. Serum samples were aliquoted, de-identified,
137 and classified as IgM-positive/IgG-negative, IgM-positive/IgG-positive, or IgM-negative/IgG-
138 positive, based on the Western blot results. Post-treatment Lyme disease (PTLD) serum samples
139 (n=158) were kindly provided by the Lyme Disease Biobank at Nuvance Health® (Danbury, CT).
140 PTLD was defined as described by Aucott (8).
141

142 **Multiplexed OspC and OspC peptide microsphere immunoassays (MIA).** Recombinant
143 $OspC_A$, $OspC_B$, or $OspC_K$ (5 µg) were coupled to Magplex-C microspheres (1 x 10^6) using sulfo-
144 NHS (N-hydroxysulfosuccinimide) and EDC [1-ethyl-3-(3-dimethylaminopropyl) carbodiimide
145 hydrochloride], as recommended by the manufacture (Luminex Corp., Austin, TX). Coupled
146 beads were diluted in xMap® AbC Wash Buffer to a concentration of 5 x 10^6 beads/ml. Biotin-
147 labeled peptides were complexed to Magplex®-avidin microspheres following protocols provided
148 by the manufacturer (Luminex Corp.). Microspheres were resuspended in 250 µL of assay buffer

149 (1 x PBS, 2% BSA, pH 7.4) then subjected to vortexing and sonication. A total of 1 x 10^6 beads
150 in assay buffer was mixed with biotin-conjugated peptides (~5 µg) and incubated for 30 min at
151 room temperature. The microsphere suspensions were then washed three times using wash buffer
152 (1 x PBS, 2% BSA, 0.02% TWEEN-20, 0.05% Sodium azide, pH 7.4) and a magnetic separator,
153 resuspended in 500 µL of assay buffer, and stored at 4ºC until use. For experimental use, assay
154 buffer was used to dilute bead stocks (1:50) and human serum (1:100). The bead dilution (50 µL)
155 and diluted serum (50 µL) were combined in black, clear-bottomed, non-binding, chimney 96-
156 well plates (Greiner Bio-One, Monroe, North Carolina) and allowed to incubate for 60 min in a
157 tabletop shaker (600 rpm) at room temperature. Plates were washed three times using a magnetic
158 separator and wash buffer. Secondary antibody goat anti-Human IgG Fc, eBioscience
159 (Invitrogen, Carlsbad, California) was diluted 1:500 in assay buffer and added (100 µL) to each
160 well. The secondary antibody was allowed to incubate for 30 min in a tabletop shaker (600 rpm)
161 at room temperature. Plates were washed as stated above and beads were resuspended in 100 µL
162 of wash buffer. Samples were analyzed using a FlexMap 3D (Luminex Corp.).
163
164 **Statistical analysis.** Statistical analyses were performed using R 4.3.0 with R packages readxl
165 and tidyverse (44-46). MFIs (log_{10}) were first subjected to the Shapiro-Wilk's test to assess
166 normality, then either Levene's or Fligner-Killeen tests to compare variances. Statistical
167 significance was determined by Mann-Whitney U tests with an alpha level of 0.05 using the R
168 package rstatix [https://CRAN.R-project.org/package=rstatix]. R package corrplot (47) was used
169 to generate the Spearman's Rank correlation matrix. R package pheatmap was used to create the
170 hierarchically clustered heatmaps (48). R packages ggthemes
171 [https://github.com/jrnold/ggthemes], RColorBrewer [https://cran.r-
172 project.org/web/packages/RcolorBrewer/index.html], and ggpubr [https://CRAN.R-
173 project.org/package=ggpubr] were used in formatting.
174
175 **Molecular modeling.** PyMol (DeLano Scientific LLC, Palo Alto, CA) was used for epitope
176 modeling using OspC PDB ID: **1GGQ** (strain B31, $OspC_A$).
177
178 **RESULTS**

179 We sought to validate the reactivity of OspC linear B cell epitopes, including those
180 already accessioned in the Immune Epitope Database (iedb.org), that have been directly or
181 indirectly implicated in Lyme disease diagnostics and/or immunity to *B. burgdorferi*. Eight
182 different epitopes, including the C10 peptide, were chosen for analysis **(Table 1)**. When localized
183 onto the structure of $OspC_A$ using PyMol, the epitopes represent ~30% of the surface area of the
184 molecule (**Figure 1A**). An alignment of the primary amino acid sequences of the three OspC
185 types (A, B, K) associated with invasive disease in northeast United States revealed
186 polymorphisms in a number of these epitopes (**Table 1**; **Figure 1B**) (49, 50). For this reason, a
187 total of 13 different peptides were generated to encompass the specific amino acid sequences for
188 each epitope within $OspC_A$, $OspC_B$, and $OspC_K$ (**Table 1**). The peptides were synthesized with a
189 C-terminal biotin tag and coupled to streptavidin-coated microspheres for multiplex
190 immunoassays (MIA) by Luminex. As a positive control, we also coupled microspheres with the
191 VlsE C6 B31-17 peptide from *B. burgdorferi* strain B31(43).
192 We employed two *B. burgdorferi* seropositive serum sample collections to gauge the
193 relative reactivity of recombinant OspC, OspC-derived peptides, and the VlsE C6-17 peptide. A
194 "diagnostic" collection consisted of 696 de-identified human serum samples from the Wadsworth
195 Center's Diagnostic Immunology laboratory classified as *B. burgdorferi* seropositive and
196 categorized based on Western blot banding profiles, as IgM^+/IgG^- (+/-), IgM^+/IgG^+ (+/+), or IgM^-
197 $/IgG^+$ (-/+). A second collection provided by the Lyme Disease Biobank at Nuvance Health
198 consisted of 158 serum samples from PTLD patients. These two collections were compared to a
199 commercial panel consisting of ~75 serum samples confirmed negative for VlsE C6-17 peptide
200 reactivity. Reactivity was limited to IgG analysis, since preliminary IgM reactivity profiles were
201 low or inconclusive for the two sample sets (data not shown).
202 We found that the diagnostic immunology samples were significantly more reactive with
203 recombinant OspC than the control samples, although reactivity was skewed towards $OspC_A$ and
204 $OspC_B$ more than $OspC_K$ **(Figure 2A)**. We can only speculate that this bias reflects actual
205 exposure to *B. burgdorferi* expressing these two OspC types. In terms of peptides, the diagnostic
206 serum samples were on average significantly more reactive than control serums samples with all
207 the OspC-derived peptides tested, except for peptides $71\text{-}86_A$ and $178\text{-}187_B$ (**Figure 2A**). The
208 average serum IgG reactivity was highest against C10 ($193\text{-}210_A$) and VlsE C6-17 ($p<0.0001$)
209 with the remainder of the peptides being low to moderately reactive relative to the control.

210 To apply a more rigorous test of peptide reactivity, MFI values were subjected to a cutoff
211 value of ≥6 SD above the mean of the control MFI, log_{10} transformed, then plotted to reveal both
212 the number of serum samples above the cutoff (% positive) as well as the magnitude of samples
213 over the cutoff (fold increase). We also derived box and whisker plots to illustrate the upper and
214 lower quartiles as well as the median reactivity to each antigen/peptide with superimposed violin
215 plots to outline sample distribution. Using these metrics, reactivity with $OspC_A$, $OspC_B$ and
216 $OspC_K$ ranged from 24-42% of the diagnostic samples with the fold increase ranging from 2.8 to
217 4.7 (**Table 2**; **Figure 3A**). In terms of peptides, VlsE C6-17 was the most reactive (71% positive;
218 fold increase 5.8), followed by peptide C10 (26% positive; fold increase 4.4) (**Table 3; Figure**
219 **3B**). The percent of samples >6SD for the other 12 peptides ranged from 0.1 to 10% with the
220 fold increase between 1.2 and 2.5 (**Table 3; Figure 3B**). Thus, while overall MFI values
221 indicating that OspC peptides are widely recognized by *B. burgdorferi* immune sera, applying a
222 more stringent threshold to the analysis suggests a different story. Namely, that OspC-derived
223 peptides (apart from C10) are recognized by only a fraction of the total diagnostic serum
224 samples. While the profile suggests limited utility of peptides other than C10 for diagnostic
225 applications, it does raise questions about whether reactivity with particular linear epitopes on
226 OspC influence disease outcome, a point that we will return to in the Discussion.
227 The same overall serologic analysis was performed with a panel of PTLD samples. The
228 PTLD samples were significantly more reactive with $OspC_A$, $OspC_B$ and $OspC_K$ than the control
229 serum samples (**Figure 2B**). For $OspC_A$ and $OspC_K$, 16 and 18% of the samples were above the
230 ≥6SD cutoff with the fold increase between 2.8-5 (**Table 2; Figure 3C**). In the case of $OspC_B$,
231 only 3.2% were above the cutoff with a fold increase of 2.1 (**Table 2; Figure 3C**). In terms of
232 linear epitopes, reactivity significantly above controls was limited to VlsE C6-17 (40% positive;
233 fold increase 5.6), C10 (14% positive; fold increase 3.3), and $178\text{-}187_K$ (9.5%; positive; fold
234 increase 3.0) (**Figure 2B**, **Table 3, Figure 3D**). Comparatively, PTLD samples had significantly
235 less reactivity to peptide $9\text{-}33_{ABK}$ relative to controls (**Figure 2B**). Only a small fraction of the
236 PTLD serum samples were found to be positive for the remaining 10 peptides (range 1.3-9.5%)
237 and the MFIs did not achieve statistical significance (**Table 3, Figure 2B**). PTLD samples were
238 plotted to visualize OspC and peptide reactivities relative to the cutoff (**Figure 3C-D**). There is
239 notably less reactivity to both C10 and C6-17 in the PTLD cohort in comparison to the
240 diagnostic population (**Figure 3B, 3D**).

241 Understanding the relationships between OspC and OspC-derived peptide epitopes has
242 implications for Lyme disease diagnostics and possibly immunity to *B. burgdorferi*. We expected
243 that antibody reactivity with the OspC-derived peptides would strongly correlate with overall
244 OspC antibody levels in any given sample, suggesting that the two populations track with each
245 other and serve as redundant indicators of a previous *B. burgdorferi* infection. To investigate
246 these relationships, we generated correlation matrices (Spearman's Rank) showing the
247 correlation between OspC and the each of the different OspC-derived peptides, including C10
248 and C6-17 (**Figure 4**). While all correlations were determined to be positive, in the diagnostic
249 samples, C10 reactivity was only weakly correlated with $OspC_A$, $OspC_B$, or $OspC_K$ [r_s = 0.2-0.4]
250 (**Figure 4A**). Rather, C10 reactivity was moderately to strongly correlated with other OspC-
251 derived peptides, including $132\text{-}146_A$ (r_s = 0.63), $183\text{-}190_{AB}$ (r_s = 0.58), and $40\text{-}55_{ABK}$ (r_s = 0.58).
252 Indeed, inter-peptide correlations were generally strong across the board (e.g., $132\text{-}146_B$ versus
253 $177\text{-}186_A$, r_s >0.9). A similar pattern was observed in the PTLD samples: OspC-derived peptide
254 reactivities were strongly correlated with each other (r_s = 0.63-0.98), but weakly correlated with
255 $OspC_A$, $OspC_B$, and $OspC_K$ (r_s = 0.2-0.4) (**Figure 4B**). In the case of VlsE C6-17, reactivity was
256 weakly correlated with OspC and OspC-derived peptides in both the diagnostic and PTLD
257 samples, except for moderate correlativity with C10 in the PTLD cohort (r_s = 0.56). These results
258 reveal a significant degree of discordance (asynchrony) among circulating antibody levels
259 against OspC, OspC-derived peptides and the VlsE C6-17 peptide in both diagnostic and PTLD
260 cohorts.
261 The absence of a strong correlation between antibody levels to OspC and OspC-derived
262 peptides led us to subject the diagnostic and PTLD datasets to hierarchical clustering (HC) as
263 means to identify possible relationships in immunoreactivity profiles. In the case of the
264 diagnostic samples, the horizontal (top) dendrogram revealed three distinct branches consisting
265 of (1) $OspC_A$, $OspC_B$, and $OspC_K$, (2) C6-17 and C10, and (3) the other OspC-derived peptides
266 (**Figure 5A**). In cluster 1 ($OspC_A$, $OspC_B$, $OspC_K$), high MFI values were distributed throughout
267 the column with a concentration towards the lower quartile. There was no obvious clustering on
268 the vertical dendrogram to indicate a relationship between OspC reactivity and seropositivity
269 categories (i.e., $IgM^{+/-}$, $IgG^{+/-}$).
270 In branch 2, high VlsE C6-17 reactivity was present throughout the column, albeit, with
271 three hot (orange and red shading) zones and one cold (deep blue shading) zone. In the C10

272 column, there was generally an even distribution of MFI intensities only occasionally punctuated
273 with hot spots that often mirror C10 reactivity. Samples that were "cold" for C6-17 and C10
274 tended to be within the IgM+/IgG- pool, possibly indicative of an early response to *B.*
275 *burgdorferi* infection.

276 There were several interesting patterns within branch 3, which consisted of OspC-derived
277 peptides: uniformly low reactivity with peptide 9-33$_{ABK}$, as noted in Figures 2 and 3; a
278 subpopulation of samples that were uniformly nonreactive with all the OspC peptides, as
279 evidenced by a blue band across the top of the figure, which in some instances spilled over to
280 C10 and VlsE C6-17 columns; and, finally, a subpopulation of samples with moderate to high
281 pan-OspC peptide reactivity, as evidenced by a horizontal band of orange/red shading situated in
282 the lower third of the figure. Collectively, the HC analysis reveals a remarkable degree of
283 discordance in serum antibody profiles associated with *B. burgdorferi* seropositivity within the
284 diagnostic samples.

285 The HC plot of the PTLD serum samples was clearly distinct from the diagnostic samples
286 (**Figure 5B**). On the horizontal dendrogram, for example, there were just two major branches not
287 three: one encompassing OspC$_{ABK}$ and C6-17, and the other containing the OspC-derived
288 peptides, including C10. On the vertical dendrogram, there were two branches: the top branch
289 corresponding to low peptide reactivity with or without concomitant C6-17 and OspC
290 reactivities; and the bottom branch corresponding to high peptide reactivity that were more
291 frequently than not associated with high C6-17 reactivity. Within the bottom branch, there was a
292 notable subbranch corresponding to 4 samples with strikingly high reactivity with C10, C6-17,
293 and most of the OspC-derived peptides (including 9-33$_{ABK}$). We would tentatively classify these
294 handful of samples as "polyreactive" (51).

295 **Contribution of C10 to overall OspC antibody reactivity**. There is some debate as to
296 what proportion C10-specific antibodies constitute relative to total OspC antibodies, with some
297 studies reporting that C10-specific antibodies make up an overwhelming proportion (52), while
298 others suggesting the opposite (53). As our prior analysis included truncated derivatives of OspC
299 that lacked C10, we expressed a second version of OspC in which residues 202-210
300 (VVAESPKKP) were included. We then revisited Luminex analysis in which we compared MFI
301 to OspC$_A$ versus OspC$_A$+C10. MFIs for OspC$_A$+C10 were significantly greater than OspC$_A$ in
302 both diagnostic and PTLD cohorts, demonstrating that antibody reactivity to the conserved C-

303 terminal residues constitute an important component of the overall antibody response ($p < 0.05$;
304 Mann-Whitney U test) (**Figure 6A, Figure 6D**). We then investigated the relationship between
305 C10 reactivity and $OspC_A$ vs $OspC_A$+C10 using a linear regression model for diagnostic samples
306 (**Figure 6B, Figure 6C**) and PTLD samples (**Figure 6E, Figure 6F**). There is a slight increase
307 (0.0702) in the adjusted R-squared value between the C10 peptide MFI and $OspC_A$+C10, as
308 compared to $OspC_A$ for the DI cohort (**Figure 6B, Figure 6C**). A similar increase (0.0848) in the
309 adjusted R-squared value was observed between the C10 peptide and $OspC_A$+C10 in comparison
310 to $OspC_A$ for the PTLD population. However, the overall adjusted R-squared value was
311 negligible, thereby demonstrating that C10-specific antibodies constitute only a small fraction of
312 the total OspC reactivity.
313
314 **DISCUSSION**
315 Defining the breadth and the frequency of linear B cell epitope reactivity on OspC has
316 important implications for both Lyme disease diagnostics and vaccines. In this report, a panel of
317 peptides representing eight previously reported and predicted linear epitopes on OspC types A, B
318 and K, were examined by multiplex immunoassay for serum IgG reactivity in diagnostic (n~700)
319 and PTLD (n~150) *B. burgdorferi* seropositive sample sets. The results revealed that seven of the
320 eight peptides are indeed antibody targets even though reactivity to any given peptide may be
321 confined to a fraction (2-10%) of the total samples tested. The exception being peptide C10,
322 which was 26% positive (4.4 positive fold increase value) in the diagnostic sample set and 14%
323 positive (3.3 positive fold increase value) in the PLTDs sample set. Interestingly, in the
324 diagnostic sample set, C10 antibody titers did not correlate with either reactivity to OspC itself or
325 any of the other OspC-derived peptides. In the PTLD sample set, C10 antibody levels did
326 correlate with the other OspC-derived peptides but were distinct from OspC. These results have
327 clinical implications, as they demonstrate that the human B cell response to linear epitopes on
328 OspC is both variable and asynchronous.
329 The C10 peptide corresponds to the stretch of ~10 highly conserved amino acids at C-
330 terminus of OspC, first recognized as an immunodominant epitope in neuroborreliosis patients
331 (52). Since then, the C10 peptide and derivatives have been integrated into numerous diagnostic
332 assays, including the Zeus VlseE1/C10 ELISA (25, 27, 28). Dolange and colleagues recently
333 proposed the use of high affinity C10-specific monoclonal antibodies as tools to detect

334 circulating levels of *B. burgdorferi* antigens (54). While there is little debate as to whether C10
335 constitutes a human B cell epitope, the issue of whether antibodies to C10 contribute to
336 borreliacidal activity remains contentious. Lovrich and colleagues reported that OspC-specific
337 borreliacidal activity (in a handful of human serum samples) was almost entirely directed against
338 C10 (55, 56), whereas Izac and colleagues argued that, in rodents, canines and non-human
339 primates, C10-specific antibodies contribute little if any borreliacidal activity (57). Although our
340 results do not resolve this issue per se, they do raise questions about the underlying B cell
341 biology associated with antibodies to C10 and OspC. The fact that C10 and OspC antibody titers
342 did not correlate with each other in the two serum sample sets examined suggests differences in
343 the kinetics of antibody induction, circulating half-life, and/or plasma cell persistence. Others
344 have suggested, at least in the case of VlsE, there is a distinct progression of epitope reactivity
345 over the course of *B. burgdorferi* infection with readily accessible epitopes targeted first and
346 more obstructed, membrane proximal epitopes following (58). Resolving detailed questions
347 about the nature of the human B cell response to OspC is becoming more feasible as single cell
348 V_H and V_L repertoires are catalogued over the course of Lyme disease (11, 59).
349 B cell epitope prediction software like Discotope 3.0 identifies residues 133-147 as
350 having a high immunogenic propensity (60). That prediction was borne out in our study, as
351 evidenced by statistically significant reactivity of serum samples with the three peptides
352 corresponding to residues $132\text{-}146_{AB}$ and $133\text{-}147_{K}$. Others have reported similar findings in
353 mice and in a few human samples. Namely, Earnhart recognized residues 136-150 (which they
354 refer to as "loop 5") as a target of antibodies in *B. burgdorferi*-infected mice (36). In a follow-up
355 study, the same investigators identified two serum samples from early Lyme disease patients that
356 reacted with peptides spanning 136-144 (61). A subsequent report by Arnaboldi and colleagues
357 did not detect binding to three different 15-mer $OspC_K$-derived peptides spanning residues 131-
358 155, possibly because their sample size was limited (27). In our collection of almost 700
359 diagnostic samples, the frequency of peptide positivity was admittedly relatively low (3-7%).
360 Nonetheless, antibodies targeting this epitopic region may be consequential in terms of
361 promoting spirochete clearance (36). For example, the potent borreliacidal mouse monoclonal
362 antibody 16.22 recognizes $OspC_A$ residues 133-147 with the key contact points postulated to be
363 residues 139-141 ("KXK" motif) (62). Thus, a more detailed examination of B cell epitopes
364 within this region of OspC in human Lyme disease patients is warranted.

365 It has been postulated that serum antibody profiling at the antigen and possibly even
366 epitope level may be able to resolve different stages of Lyme disease (e.g., acute, acute resolved,
367 PTLD) (10, 58). While the antibody profiling in our study was limited to serum IgG reactivity to
368 OspC, OspC-derived peptides, and VlsE C6-17, the results revealed distinct patterns between the
369 diagnostic and PTLD sample sets when subjected to HC. Most notable was the classification of
370 the C10 peptide: in the diagnostic sample set C10 clustered with C6-17, whereas in the PTLD
371 samples it clustered with the other OspC-derived peptides. Thus, it is tempting to speculate that
372 the ratio of C10 to C6-17 serum IgG reactivity may have some utility in defining disease
373 progression. By the same token, as virtually all samples tested were positive for either C10
374 and/or C6-17, establishing a combined C10 + C6-17 threshold value might serve to alleviate
375 false positives in Lyme disease diagnostics based solely on serology (63, 64). That said we
376 recognize that any claims to this effect are premature, considering that the serum samples
377 employed in our study are not associated with any clinical information beyond seropositivity.
378 Moreover, we lack a "post-Lyme healthy" cohort that Chandra and colleagues so effectively used
379 in their study to compare with their PTLD cohort (10).
380 One interesting pattern that emerged from the PTLD cohort was a cluster of four
381 individuals who demonstrated pan-reactivity with the OspC-derived peptides and VlsE C6-17
382 peptide. In follow-up analysis, those same four samples in question also reacted with other *B.*
383 *burgdorferi*-derived peptides, as well as control non-*B. burgdorferi*-derived peptides, but not
384 necessarily with the corresponding recombinant proteins (G. Freeman-Gallant, unpublished
385 results). Thus, the serum antibodies from those particular individuals seemingly have a
386 propensity for peptide antigens, possibly due to a particular bias in germline chain usage and
387 corresponding paratopes conducive to accommodating peptides (65). Whether or not there is a
388 germline bias in antibodies associated with PTLD is worthy of investigation, especially in light
389 of finding related to COVID-19. Moreover, the availability of bulk plasmablast BCR sequences,
390 as well as single cell paired BCR sequences from LD patients opens the door to detailed antibody
391 reactivity profiles and links to disease manifestations (66). We are also exploring the possibility
392 that these particular samples may have profiles consistent with autoantibodies (67) or have
393 characteristics associated with polyreactivity that might promote ligation to spirochete surface
394 antigens (68, 69).
395

Acknowledgements

We thank Dr. William Lee and other members of the Diagnostic Immunology Laboratory at the Wadsworth Center for providing residual diagnostic serum samples. We gratefully acknowledge Dr. John Martignetti and Lisa Arrigo of the Nuvance Health Lyme disease Biobank for generously providing PTLD serum samples. We thank Elizabeth Cavosie (Wadsworth Center) for administrative assistance and Greta Van Slyke (Wadsworth Center) for establishing Luminex protocols. This work was supported by the National Institute of Allergy and Infectious Diseases (NIAID), National Institutes of Health, Department of Health and Human Services, Contract No. 75N93019C00040 (PI/PD Mantis). The content is solely the responsibility of the authors and does not necessarily represent the official views of the National Institutes of Health.

Conflicts of Interest

The authors have no conflicts to declare.

References Cited

1. Kugeler KJ, Schwartz AM, Delorey MJ, Mead PS, Hinckley AF. 2021. Estimating the Frequency of Lyme Disease Diagnoses, United States, 2010-2018. Emerg Infect Dis 27:616-619.
2. Bobe JR, Jutras BL, Horn EJ, Embers ME, Bailey A, Moritz RL, Zhang Y, Soloski MJ, Ostfeld RS, Marconi RT, Aucott J, Ma'ayan A, Keesing F, Lewis K, Ben Mamoun C, Rebman AW, McClune ME, Breitschwerdt EB, Reddy PJ, Maggi R, Yang F, Nemser B, Ozcan A, Garner O, Di Carlo D, Ballard Z, Joung HA, Garcia-Romeu A, Griffiths RR, Baumgarth N, Fallon BA. 2021. Recent Progress in Lyme Disease and Remaining Challenges. Front Med (Lausanne) 8:666554.
3. Radolf JD, Strle K, Lemieux JE, Strle F. 2021. Lyme Disease in Humans. Curr Issues Mol Biol 42:333-384.
4. Steere AC, Strle F, Wormser GP, Hu LT, Branda JA, Hovius JW, Li X, Mead PS. 2016. Lyme borreliosis. Nat Rev Dis Primers 2:16090.
5. Lochhead RB, Strle K, Arvikar SL, Weis JJ, Steere AC. 2021. Lyme arthritis: linking infection, inflammation and autoimmunity. Nat Rev Rheumatol 17:449-461.

427 6. Klempner MS, Hu LT, Evans J, Schmid CH, Johnson GM, Trevino RP, Norton D, Levy
428 L, Wall D, McCall J, Kosinski M, Weinstein A. 2001. Two controlled trials of antibiotic
429 treatment in patients with persistent symptoms and a history of Lyme disease. N Engl J
430 Med 345:85-92.
431 7. Marques A. 2008. Chronic Lyme disease: a review. Infect Dis Clin North Am 22:341-60,
432 vii-viii.
433 8. Aucott JN, Crowder LA, Kortte KB. 2013. Development of a foundation for a case
434 definition of post-treatment Lyme disease syndrome. Int J Infect Dis 17:e443-9.
435 9. Aucott JN, Yang T, Yoon I, Powell D, Geller SA, Rebman AW. 2022. Risk of post-
436 treatment Lyme disease in patients with ideally-treated early Lyme disease: A prospective
437 cohort study. Int J Infect Dis 116:230-237.
438 10. Chandra A, Wormser GP, Marques AR, Latov N, Alaedini A. 2011. Anti-Borrelia
439 burgdorferi antibody profile in post-Lyme disease syndrome. Clin Vaccine Immunol
440 18:767-71.
441 11. Blum LK, Adamska JZ, Martin DS, Rebman AW, Elliott SE, Cao RRL, Embers ME,
442 Aucott JN, Soloski MJ, Robinson WH. 2018. Robust B Cell Responses Predict Rapid
443 Resolution of Lyme Disease. Front Immunol 9:1634.
444 12. Bockenstedt LK, Wooten RM, Baumgarth N. 2021. Immune Response to Borrelia: Lessons
445 from Lyme Disease Spirochetes. Curr Issues Mol Biol 42:145-190.
446 13. Embers ME, Hasenkampf NR, Jacobs MB, Philipp MT. 2012. Dynamic longitudinal
447 antibody responses during Borrelia burgdorferi infection and antibiotic treatment of rhesus
448 macaques. Clin Vaccine Immunol 19:1218-26.
449 14. Jiang R, Meng H, Raddassi K, Fleming I, Hoehn KB, Dardick KR, Belperron AA,
450 Montgomery RR, Shalek AK, Hafler DA, Kleinstein SH, Bockenstedt LK. 2021. Single-
451 cell immunophenotyping of the skin lesion erythema migrans identifies IgM memory B
452 cells. JCI Insight 6.
453 15. Barbour AG, Jasinskas A, Kayala MA, Davies DH, Steere AC, Baldi P, Felgner PL. 2008.
454 A genome-wide proteome array reveals a limited set of immunogens in natural infections
455 of humans and white-footed mice with Borrelia burgdorferi. Infect Immun 76:3374-89.

456 16. Tilly K, Krum JG, Bestor A, Jewett MW, Grimm D, Bueschel D, Byram R, Dorward D,
457 Vanraden MJ, Stewart P, Rosa P. 2006. Borrelia burgdorferi OspC protein required
458 exclusively in a crucial early stage of mammalian infection. Infect Immun 74:3554-64.
459 17. Pal U, Yang X, Chen M, Bockenstedt LK, Anderson JF, Flavell RA, Norgard MV, Fikrig
460 E. 2004. OspC facilitates Borrelia burgdorferi invasion of Ixodes scapularis salivary
461 glands. J Clin Invest 113:220-30.
462 18. Tilly K, Bestor A, Jewett MW, Rosa P. 2007. Rapid clearance of Lyme disease spirochetes
463 lacking OspC from skin. Infect Immun 75:1517-9.
464 19. Earnhart CG, Leblanc DV, Alix KE, Desrosiers DC, Radolf JD, Marconi RT. 2010.
465 Identification of residues within ligand-binding domain 1 (LBD1) of the Borrelia
466 burgdorferi OspC protein required for function in the mammalian environment. Mol
467 Microbiol 76:393-408.
468 20. Caine JA, Coburn J. 2016. Multifunctional and Redundant Roles of Borrelia burgdorferi
469 Outer Surface Proteins in Tissue Adhesion, Colonization, and Complement Evasion. Front
470 Immunol 7:442.
471 21. Caine JA, Lin YP, Kessler JR, Sato H, Leong JM, Coburn J. 2017. Borrelia burgdorferi
472 outer surface protein C (OspC) binds complement component C4b and confers bloodstream
473 survival. Cell Microbiol 19.
474 22. Lin YP, Tan X, Caine JA, Castellanos M, Chaconas G, Coburn J, Leong JM. 2020. Strain-
475 specific joint invasion and colonization by Lyme disease spirochetes is promoted by outer
476 surface protein C. PLoS Pathog 16:e1008516.
477 23. Tan X, Castellanos M, Chaconas G. 2023. Choreography of Lyme Disease Spirochete
478 Adhesins To Promote Vascular Escape. Microbiol Spectr 11:e0125423.
479 24. Branda JA, Steere AC. 2021. Laboratory Diagnosis of Lyme Borreliosis. Clin Microbiol
480 Rev 34.
481 25. Hahm JB, Breneman JWt, Liu J, Rabkina S, Zheng W, Zhou S, Walker RP, Kaul R. 2020.
482 A Fully Automated Multiplex Assay for Diagnosis of Lyme Disease with High Specificity
483 and Improved Early Sensitivity. J Clin Microbiol 58.
484 26. Bacon RM, Biggerstaff BJ, Schriefer ME, Gilmore RD, Jr., Philipp MT, Steere AC,
485 Wormser GP, Marques AR, Johnson BJ. 2003. Serodiagnosis of Lyme disease by kinetic
486 enzyme-linked immunosorbent assay using recombinant VlsE1 or peptide antigens of

487 Borrelia burgdorferi compared with 2-tiered testing using whole-cell lysates. J Infect Dis
488 187:1187-99.
489 27. Arnaboldi PM, Seedarnee R, Sambir M, Callister SM, Imparato JA, Dattwyler RJ. 2013.
490 Outer surface protein C peptide derived from Borrelia burgdorferi sensu stricto as a target
491 for serodiagnosis of early lyme disease. Clin Vaccine Immunol 20:474-81.
492 28. Baarsma ME, Vrijlandt A, Ursinus J, Zaaijer HL, Jurriaans S, van Dam AP, Hovius JW.
493 2022. Diagnostic performance of the ZEUS Borrelia VlsE1/pepC10 assay in European LB
494 patients: a case-control study. Eur J Clin Microbiol Infect Dis 41:387-393.
495 29. Coleman AS, Rossmann E, Yang X, Song H, Lamichhane CM, Iyer R, Schwartz I, Pal U.
496 2011. BBK07 immunodominant peptides as serodiagnostic markers of Lyme disease. Clin
497 Vaccine Immunol 18:406-13.
498 30. Mathiesen MJ, Christiansen M, Hansen K, Holm A, Asbrink E, Theisen M. 1998. Peptide-
499 based OspC enzyme-linked immunosorbent assay for serodiagnosis of Lyme borreliosis. J
500 Clin Microbiol 36:3474-9.
501 31. O'Bier NS, Hatke AL, Camire AC, Marconi RT. 2021. Human and Veterinary Vaccines
502 for Lyme Disease. Curr Issues Mol Biol 42:191-222.
503 32. Wilske B, Preac-Mursic V, Jauris S, Hofmann A, Pradel I, Soutschek E, Schwab E, Will
504 G, Wanner G. 1993. Immunological and molecular polymorphisms of OspC, an
505 immunodominant major outer surface protein of Borrelia burgdorferi. Infect Immun
506 61:2182-91.
507 33. Barbour AG, Travinsky B. 2010. Evolution and distribution of the ospC Gene, a
508 transferable serotype determinant of Borrelia burgdorferi. MBio 1.
509 34. Cerar T, Strle F, Stupica D, Ruzic-Sabljic E, McHugh G, Steere AC, Strle K. 2016.
510 Differences in Genotype, Clinical Features, and Inflammatory Potential of Borrelia
511 burgdorferi sensu stricto Strains from Europe and the United States. Emerg Infect Dis
512 22:818-27.
513 35. Seinost G, Dykhuizen DE, Dattwyler RJ, Golde WT, Dunn JJ, Wang IN, Wormser GP,
514 Schriefer ME, Luft BJ. 1999. Four clones of Borrelia burgdorferi sensu stricto cause
515 invasive infection in humans. Infect Immun 67:3518-24.
516 36. Earnhart CG, Buckles EL, Dumler JS, Marconi RT. 2005. Demonstration of OspC type
517 diversity in invasive human lyme disease isolates and identification of previously

518 uncharacterized epitopes that define the specificity of the OspC murine antibody response.
519 Infect Immun 73:7869-77.
520 37. Hanincova K, Mukherjee P, Ogden NH, Margos G, Wormser GP, Reed KD, Meece JK,
521 Vandermause MF, Schwartz I. 2013. Multilocus sequence typing of Borrelia burgdorferi
522 suggests existence of lineages with differential pathogenic properties in humans. PLoS One
523 8:e73066.
524 38. Fraser CM, Casjens S, Huang WM, Sutton GG, Clayton R, Lathigra R, White O, Ketchum
525 KA, Dodson R, Hickey EK, Gwinn M, Dougherty B, Tomb JF, Fleischmann RD,
526 Richardson D, Peterson J, Kerlavage AR, Quackenbush J, Salzberg S, Hanson M, van Vugt
527 R, Palmer N, Adams MD, Gocayne J, Weidman J, Utterback T, Watthey L, McDonald L,
528 Artiach P, Bowman C, Garland S, Fuji C, Cotton MD, Horst K, Roberts K, Hatch B, Smith
529 HO, Venter JC. 1997. Genomic sequence of a Lyme disease spirochaete, Borrelia
530 burgdorferi. Nature 390:580-6.
531 39. Anderson JF, Flavell RA, Magnarelli LA, Barthold SW, Kantor FS, Wallich R, Persing
532 DH, Mathiesen D, Fikrig E. 1996. Novel Borrelia burgdorferi isolates from Ixodes
533 scapularis and Ixodes dentatus ticks feeding on humans. J Clin Microbiol 34:524-9.
534 40. Steere AC, Grodzicki RL, Kornblatt AN, Craft JE, Barbour AG, Burgdorfer W, Schmid
535 GP, Johnson E, Malawista SE. 1983. The spirochetal etiology of Lyme disease. N Engl J
536 Med 308:733-40.
537 41. Rudolph MJ, Davis SA, Haque HME, Weis DD, Vance DJ, Piazza CL, Ejemel M, Cavacini
538 L, Wang Y, Mbow ML, Gilmore RD, Mantis NJ. 2023. Structural Elucidation of a
539 Protective B Cell Epitope on Outer Surface Protein C (OspC) of the Lyme Disease
540 Spirochete, Borreliella burgdorferi. mBio 14:e0298122.
541 42. Kringelum JV, Lundegaard C, Lund O, Nielsen M. 2012. Reliable B cell epitope
542 predictions: impacts of method development and improved benchmarking. PLoS Comput
543 Biol 8:e1002829.
544 43. Gomes-Solecki MJ, Meirelles L, Glass J, Dattwyler RJ. 2007. Epitope length, genospecies
545 dependency, and serum panel effect in the IR6 enzyme-linked immunosorbent assay for
546 detection of antibodies to Borrelia burgdorferi. Clin Vaccine Immunol 14:875-9.
547 44. R core Team. 2023. R: A language and environment for statistical computing. R
548 Foundation for Statistical Computing,.

549 45. Wickham H, Bryan J. 2023. Read Excel Files, v1.4.3. CRAN. https://readxl.tidyverse.org,
550 https://github.com/tidyverse/readxl.
551 46. Wickham H. 2019. Welcome to the Tidyverse. Journal of Open Source Software 4:1686.
552 47. Wei T, Simko V, Levy M, Xie Y, Jin Y, Zemla J. 2017. Package 'corrplot'. Statistician
553 56:e24.
554 48. Kolde R. 2018-05-19 2018. pheatmap: Pretty Heatmaps. https://cran.r-
555 project.org/web/packages/pheatmap/index.html. Accessed
556 49. Lemieux JE, Huang W, Hill N, Cerar T, Freimark L, Hernandez S, Luban M, Maraspin V,
557 Bogovic P, Ogrinc K, Ruzic-Sabljic E, Lapierre P, Lasek-Nesselquist E, Singh N, Iyer R,
558 Liveris D, Reed KD, Leong JM, Branda JA, Steere AC, Wormser GP, Strle F, Sabeti PC,
559 Schwartz I, Strle K. 2023. Whole genome sequencing of human Borrelia burgdorferi
560 isolates reveals linked blocks of accessory genome elements located on plasmids and
561 associated with human dissemination. PLoS Pathog 19:e1011243.
562 50. Wormser GP, Brisson D, Liveris D, Hanincova K, Sandigursky S, Nowakowski J,
563 Nadelman RB, Ludin S, Schwartz I. 2008. Borrelia burgdorferi genotype predicts the
564 capacity for hematogenous dissemination during early Lyme disease. J Infect Dis
565 198:1358-64.
566 51. Dimitrov JD, Planchais C, Roumenina LT, Vassilev TL, Kaveri SV, Lacroix-Desmazes S.
567 2013. Antibody polyreactivity in health and disease: statu variabilis. J Immunol 191:993-
568 9.
569 52. Mathiesen MJ, Holm A, Christiansen M, Blom J, Hansen K, Ostergaard S, Theisen M.
570 1998. The dominant epitope of Borrelia garinii outer surface protein C recognized by sera
571 from patients with neuroborreliosis has a surface-exposed conserved structural motif.
572 Infect Immun 66:4073-9.
573 53. Earnhart CG, Rhodes DV, Smith AA, Yang X, Tegels B, Carlyon JA, Pal U, Marconi RT.
574 2014. Assessment of the potential contribution of the highly conserved C-terminal motif
575 (C10) of Borrelia burgdorferi outer surface protein C in transmission and infectivity.
576 Pathog Dis 70:176-84.
577 54. Dolange V, Simon S, Morel N. 2021. Detection of Borrelia burgdorferi antigens in tissues
578 and plasma during early infection in a mouse model. Sci Rep 11:17368.

579 55. Jobe DA, Lovrich SD, Schell RF, Callister SM. 2003. C-terminal region of outer surface
580 protein C binds borreliacidal antibodies in sera from patients with Lyme disease. Clin
581 Diagn Lab Immunol 10:573-8.
582 56. Lovrich SD, Jobe DA, Schell RF, Callister SM. 2005. Borreliacidal OspC antibodies
583 specific for a highly conserved epitope are immunodominant in human lyme disease and
584 do not occur in mice or hamsters. Clin Diagn Lab Immunol 12:746-51.
585 57. Izac JR, Camire AC, Earnhart CG, Embers ME, Funk RA, Breitschwerdt EB, Marconi RT.
586 2019. Analysis of the antigenic determinants of the OspC protein of the Lyme disease
587 spirochetes: Evidence that the C10 motif is not immunodominant or required to elicit
588 bactericidal antibody responses. Vaccine 37:2401-2407.
589 58. Jacek E, Tang KS, Komorowski L, Ajamian M, Probst C, Stevenson B, Wormser GP,
590 Marques AR, Alaedini A. 2016. Epitope-Specific Evolution of Human B Cell Responses
591 to Borrelia burgdorferi VlsE Protein from Early to Late Stages of Lyme Disease. J Immunol
592 196:1036-43.
593 59. Kirpach J, Colone A, Burckert JP, Faison WJ, Dubois A, Sinner R, Reye AL, Muller CP.
594 2019. Detection of a Low Level and Heterogeneous B Cell Immune Response in Peripheral
595 Blood of Acute Borreliosis Patients With High Throughput Sequencing. Front Immunol
596 10:1105.
597 60. Hoie MH, Gade FS, Johansen JM, Wurtzen C, Winther O, Nielsen M, Marcatili P. 2024.
598 DiscoTope-3.0: improved B-cell epitope prediction using inverse folding latent
599 representations. Front Immunol 15:1322712.
600 61. Buckles EL, Earnhart CG, Marconi RT. 2006. Analysis of antibody response in humans to
601 the type A OspC loop 5 domain and assessment of the potential utility of the loop 5 epitope
602 in Lyme disease vaccine development. Clin Vaccine Immunol 13:1162-5.
603 62. Yang X, Li Y, Dunn JJ, Luft BJ. 2006. Characterization of a unique borreliacidal epitope
604 on the outer surface protein C of Borrelia burgdorferi. FEMS Immunol Med Microbiol
605 48:64-74.
606 63. Rebman AW, Crowder LA, Kirkpatrick A, Aucott JN. 2015. Characteristics of
607 seroconversion and implications for diagnosis of post-treatment Lyme disease syndrome:
608 acute and convalescent serology among a prospective cohort of early Lyme disease
609 patients. Clin Rheumatol 34:585-9.

610 64. Reifert J, Kamath K, Bozekowski J, Lis E, Horn EJ, Granger D, Theel ES, Shon J, Sawyer
611 JR, Daugherty PS. 2021. Serum Epitope Repertoire Analysis Enables Early Detection of
612 Lyme Disease with Improved Sensitivity in an Expandable Multiplex Format. J Clin
613 Microbiol 59.
614 65. Cobaugh CW, Almagro JC, Pogson M, Iverson B, Georgiou G. 2008. Synthetic antibody
615 libraries focused towards peptide ligands. J Mol Biol 378:622-33.
616 66. Blum JS, Fiani ML, Stahl PD. 1991. Proteolytic cleavage of ricin A chain in endosomal
617 vesicles. Evidence for the action of endosomal proteases at both neutral and acidic pH. J
618 Biol Chem 266:22091-5.
619 67. Trier NH, Houen G. 2023. Antibody Cross-Reactivity in Auto-Immune Diseases. Int J Mol
620 Sci 24.
621 68. Boughter CT, Borowska MT, Guthmiller JJ, Bendelac A, Wilson PC, Roux B, Adams EJ.
622 2020. Biochemical patterns of antibody polyreactivity revealed through a bioinformatics-
623 based analysis of CDR loops. Elife 9.
624 69. Mouquet H, Scheid JF, Zoller MJ, Krogsgaard M, Ott RG, Shukair S, Artyomov MN,
625 Pietzsch J, Connors M, Pereyra F, Walker BD, Ho DD, Wilson PC, Seaman MS, Eisen
626 HN, Chakraborty AK, Hope TJ, Ravetch JV, Wardemann H, Nussenzweig MC. 2010.
627 Polyreactivity increases the apparent affinity of anti-HIV antibodies by heteroligation.
628 Nature 467:591-5.
629 70. Ikushima M, Yamada F, Kawahashi S, Okuyama Y, Matsui K. 1999. Antibody response
630 to OspC-I synthetic peptide derived from outer surface protein C of Borrelia burgdorferi in
631 sera from Japanese forestry workers. Epidemiol Infect 122:429-33.
632 71. Pulzova L, Flachbartova Z, Bencurova E, Potocnakova L, Comor L, Schreterova E, Bhide
633 M. 2016. Identification of B-cell epitopes of Borrelia burgdorferi outer surface protein C
634 by screening a phage-displayed gene fragment library. Microbiol Immunol 60:669-677.
635 72. Tokarz R, Mishra N, Tagliafierro T, Sameroff S, Caciula A, Chauhan L, Patel J, Sullivan
636 E, Gucwa A, Fallon B, Golightly M, Molins C, Schriefer M, Marques A, Briese T, Lipkin
637 WI. 2018. A multiplex serologic platform for diagnosis of tick-borne diseases. Sci Rep
638 8:3158.

639 73. Yu Z, Carter JM, Sigal LH, Stein S. 1996. Multi-well ELISA based on independent peptide
640 antigens for antibody capture. Application to Lyme disease serodiagnosis. J Immunol
641 Methods 198:25-33.
642 74. Baum E, Randall AZ, Zeller M, Barbour AG. 2013. Inferring epitopes of a polymorphic
643 antigen amidst broadly cross-reactive antibodies using protein microarrays: a study of
644 OspC proteins of Borrelia burgdorferi. PLoS One 8:e67445.

645
646
647

648

649 **FIGURE LEGENDS**

650

651 **Figure 1. Relative location of linear epitopes on homdimeric OspC$_A$.** (**A**) Surface
652 representation of homodimeric OspC$_A$ (residues 38-201; PDB 1GGQ] with one monomer
653 (OspC) colored gray and the other, denoted with an apostrophe (OspC'), colored in charcoal. The
654 linear epitopes examined in this study are coded and numbered according to **Table 1**. Epitope 1
655 is represented as a bracket (]) on OspC', as its corresponding residues were truncated in the
656 recombinant version of OspC$_A$ used for X-ray crystal structure analysis. Similarly, only residues
657 193-201 of epitope 8 (residues 193-210) are shown because the C-terminus of OspC$_A$ was
658 truncated at position 201. Epitopes 6 and 7 overlap with the overlap colored as epitope 6. (**B**)
659 The same image of homodimeric OspC$_A$ as Panel A except that amino acid differences between
660 OspC types A, B and K within the eight epitopes are colored red to illustrate degree of
661 polymorphisms.

662

663 **Figure 2. Serum IgG reactivity of diagnostic and PTLD samples with OspC and OspC-**
664 **derived peptides.** (**A**) DI and (**B**) PTLD serum samples (diluted 1:100) were subject to MIA
665 using microspheres coated with recombinant dimeric OspC types A, B and K (top rows), OspC-
666 peptides as described in Table 1, and C6-17 peptide. Panels are labeled by corresponding residue
667 numbers for each OspC type. MFI values were $\log_{10}$ transformed and compared to the control
668 sample set. Significance was determined by the Mann-Whitney U-test (*, $p < 0.05$).

669

670 **Figure 3. Indexed (>6SD) IgG reactivity of DI and PTLD serum samples with OspC and**
671 **OspC-derived peptides.** MFI values for OspC and OspC- and VlsE-derived peptides were
672 indexed using a cutoff of 6SD above mean control reactivity. The resulting values were then
673 $\log_{10}$ transformed with each point representing a single sample. OspC subtypes are listed along
674 the x-axis, residues are indicated along the top of the plot (**B**, **D**), and each antigen is represented
675 by a different color. In each of the graphs, the 6 SD cutoff corresponds to a value of 0 on the y-
676 axis and is depicted with horizontal red line. All samples falling above y = 0 were found to be
677 positive for the given antigen and were used to calculate percent positivity and fold increase as
678 reported in Tables 2 and 3. Box and whisker plots illustrate the upper and lower quartiles as well

679 as the median reactivity to each antigen (thick center line). Sample points that fall above or
680 below the whiskers are considered outliers. Violin plots outline the distribution of data.
681
682 **Figure 4. Correlation matrices of rOspC and OspC-derived peptide reactivity in diagnostic**
683 **and PTLD serum.** Diagnostic (**A**) and PTLD (**B**) serum sample MFIs (indexed and $\log_{10}$
684 transformed) were subjected to Spearman's Rank correlation. Only significant correlation
685 coefficients (r_s) are displayed (confidence level = 0.95). The degree and direction of correlation is
686 indicated by the color scale. Interpretations of the strength of each correlation was conducted as
687 such: >0.7 indicates a strong correlation, 0.5 – 0.7 is moderate, 0.3 – 0.5 is weak, and 0.0 – 0.3 is
688 negligible.
689
690 **Figure 5. Hierarchical clustering of rOspC and OspC-derived reactivity in diagnostic and**
691 **PTLD serum.** Heatmaps were generated using diagnostic (**A**) and PTLD (**B**) serum sample MFIs
692 (indexed and $\log_{10}$ transformed). Rows represent individual samples and columns represent the
693 panel of antigens. The color scales of **A** and B are identical to one another (allowing for direct
694 comparison), with 0 representing the positivity cutoff (as seen in **Figure 3**). Annotation of the
695 diagnostic samples (**A**) with Western blot profile data (previously described in the Materials and
696 Methods) is designated by the legend. The columns were subjected to hierarchical clustering by
697 correlation and the rows were clustered by Euclidean distance to better visualize patterns in
698 reactivity profiles.
699
700 **Figure 6: Correlation between $OspC_A$ reactivity and C10 region.** Diagnostic (n=686) and
701 PTLD (n=158) samples were subjected to Luminex with $OspC_A$, $OspC_A$+C10, and $193\text{-}210_A$ as
702 described in the Materials and Methods. $OspC_A$ MFIs were evaluated against $OspC_A$+C10 for
703 diagnostic **(A)** and PTLD **(D)** samples. Significance was determined by Mann-Whitney U test. *,
704 $p < 0.05$. To examine the contribution of the C10 region to $OspC_A$ reactivity, MFIs for peptide
705 $193\text{-}210_A$ were plotted (on the y-axis) versus MFIs from $OspC_A$ and $OspC_A$+C10 (on the x-axis)
706 for diagnostic samples **(B, C)** and PTLD samples **(E, F)**. Best fit lines and confidence intervals
707 (level = 0.95) were added to each plot using a linear regression model. Adjusted R-squared (r^2)
708 values were calculated in R.

709 **TABLES**

710

Table 1. OspC and VlsE-derived peptides used in this study

#[a]	residues	OspC type sequence	IEDB ID [b]	References
1	9-33	ILMTLFLFISCNNSGKDGNTSANSA	181204 745120	(70) (27) (71) (72)
2	40-55	A/B–PNLTEISKKITDSNAV K–PNLTEISKKITESNAV	559957	(71)
3	71-86	A–EIAAKAIGKKIHQNNG	12383	(73)
4	132-146 132-146 133-147	A–ETFTNKLKEKHTDLG B–EEFSTKLKDNHAQLG K–EDFTKKLEGEHAQLG	63756 ,745097 14380, 18025	(62)
5	155-169	A–AKEAILKTNGTKTKG	558968 181187	(27) (71)
6	177-186 178-187 178-187	A–FESVEVLSKA B–SGSLESLSKA K–FKAVENLAKA	NA	(74)
7	183-190[c]	A/B–LSKAAKEM	560173	(71)
8	193-210	A–NSVKELTSPVVAESPKKP	745122	(25, 52, 71, 72)
C6	VlsE C6-17	MKKDDQIAAAIALRGMA	41843	(43)

[a], Numbers correspond to peptides highlighted in Figure 1, except C6. [b], Immune Epitope Database (IEDB.org) identifier. [c], Residues 184-191 in Type B.

711

712

713

714

Table 2: Serum reactivity greater than 6SD to $OspC_{A/B/K}$ in diagnostic and PTLD samples

	Diagnostic		PTLD	
OspC	**n = (%)**[a]	**Fold increase (SD)**[b]	**n = (%)**[a]	**Fold increase (SD)**[b]
A	167 (24.0)	2.8 (1.9)	29 (18.4)	5.5 (5.6)
B	287 (41.2)	3.7 (3.4)	5 (3.2)	2.1 (0.6)
K	195 (28.0)	4.7 (4.3)	26 (16.5)	2.8 (2.2)

[a], The number of samples (n =) and percent reactivity ("%") to each antigen in the diagnostic (n=696) and PTLD (n=158) sample sets were calculated using a cutoff of >6SD above the mean of controls samples; [b], The fold increase (magnitude) of positive sample antibody reactivity over controls such than an index value of 1 is 6SD above the control mean, while 2.8 corresponds to ~16SD greater than the mean control.

715

716

Table 3: Serum reactivity greater than 6SD to OspC peptides in diagnostic and PTLD serum samples

	Diagnostic		PTLD	
Peptide	**n = (%)[a]**	**Fold increase (SD)[b]**	**n = (%)[a]**	**Fold increase (SD)[b]**
$9\text{-}33_{ABK}$	1 (0.1)	2.4 (N/A)	0 (0)	N/A (N/A)
$40\text{-}55_{AB}$	17 (2.4)	2.1 (1.4)	4 (2.5)	1.6 (0.5)
$40\text{-}55_{K}$	7 (1.0)	1.5 (0.5)	2 (1.3)	1.3 (0.2)
$71\text{-}86_{A}$	28 (4.0)	1.7 (0.8)	1 (0.6)	1.4 (NA)
$132\text{-}146_{A}$	18 (2.6)	2.4 (1.5)	5 (3.2)	1.7 (0.6)
$132\text{-}146_{B}$	48 (6.9)	2.0 (1.3)	11 (7.0)	3.0 (1.9)
$133\text{-}147_{K}$	36 (5.2)	2.4 (2.6)	8 (5.1)	2.5 (1.2)
$155\text{-}169_{A}$	30 (4.3)	2.5 (2.5)	5 (3.2)	2.5 (1.5)
$177\text{-}186_{A}$	38 (5.5)	1.6 (0.7)	13 (8.2)	2.6 (2.0)
$178\text{-}187_{K}$	70 (10.1)	1.5 (0.7)	15 (9.5)	3.0 (2.8)
$178\text{-}187_{B}$	7 (1.0)	1.2 (0.1)	12 (7.6)	2.7 (1.9)
$183\text{-}190_{AB}$[c]	53 (7.6)	1.9 (1.0)	14 (8.9)	3.0 (3.1)
$193\text{-}210_{A}$ (C10)	185 (26.6)	4.4 (4.5)	22 (14.0)	3.3 (3.0)
VlsE C6-17	496 (71.3)	5.8 (2.9)	64 (40.5)	5.6 (5.0)

[a], The number of samples (n =) and percent reactivity ("%") to each antigen in the diagnostic (n=696) and PTLD (n=158) sample sets were calculated using a cutoff of >6SD above the mean of controls samples; [b], The fold increase (magnitude) of positive sample antibody reactivity over controls such than an index value of 1 is 6SD above the control mean as described in Table 2. [c], Residues 184-191 in Type B.

717

718

Figure 1

A. Putative epitopes on $OspC_A$

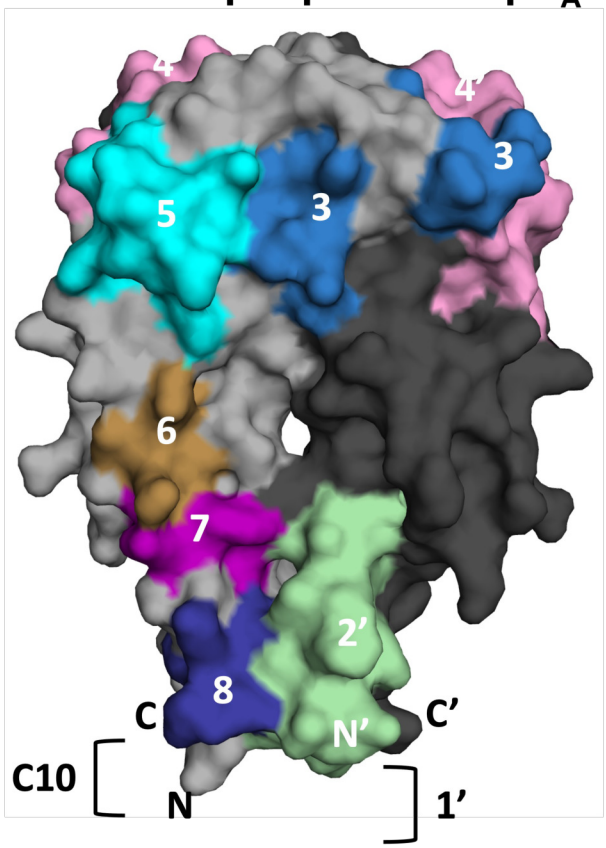

B. Polymorphisms (red) on $OspC_{A, B, K}$

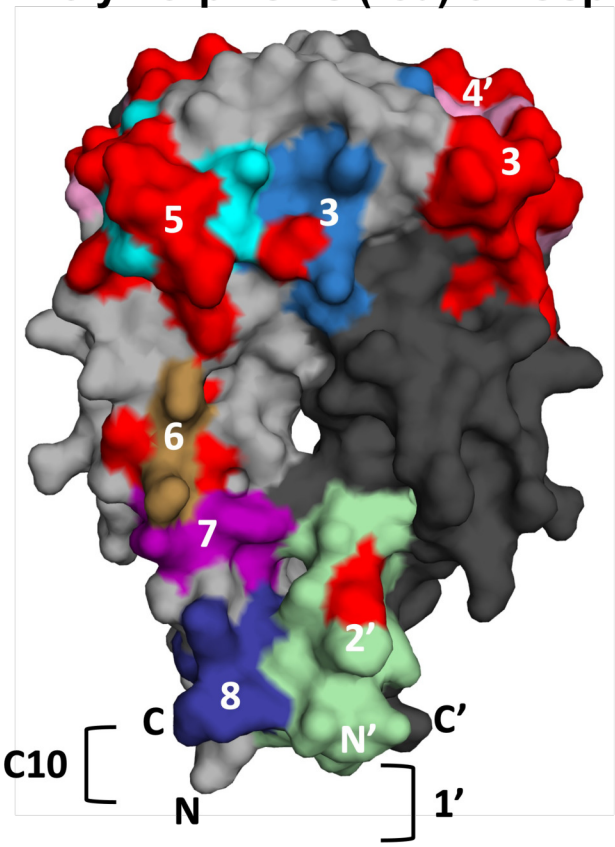

Figure 2

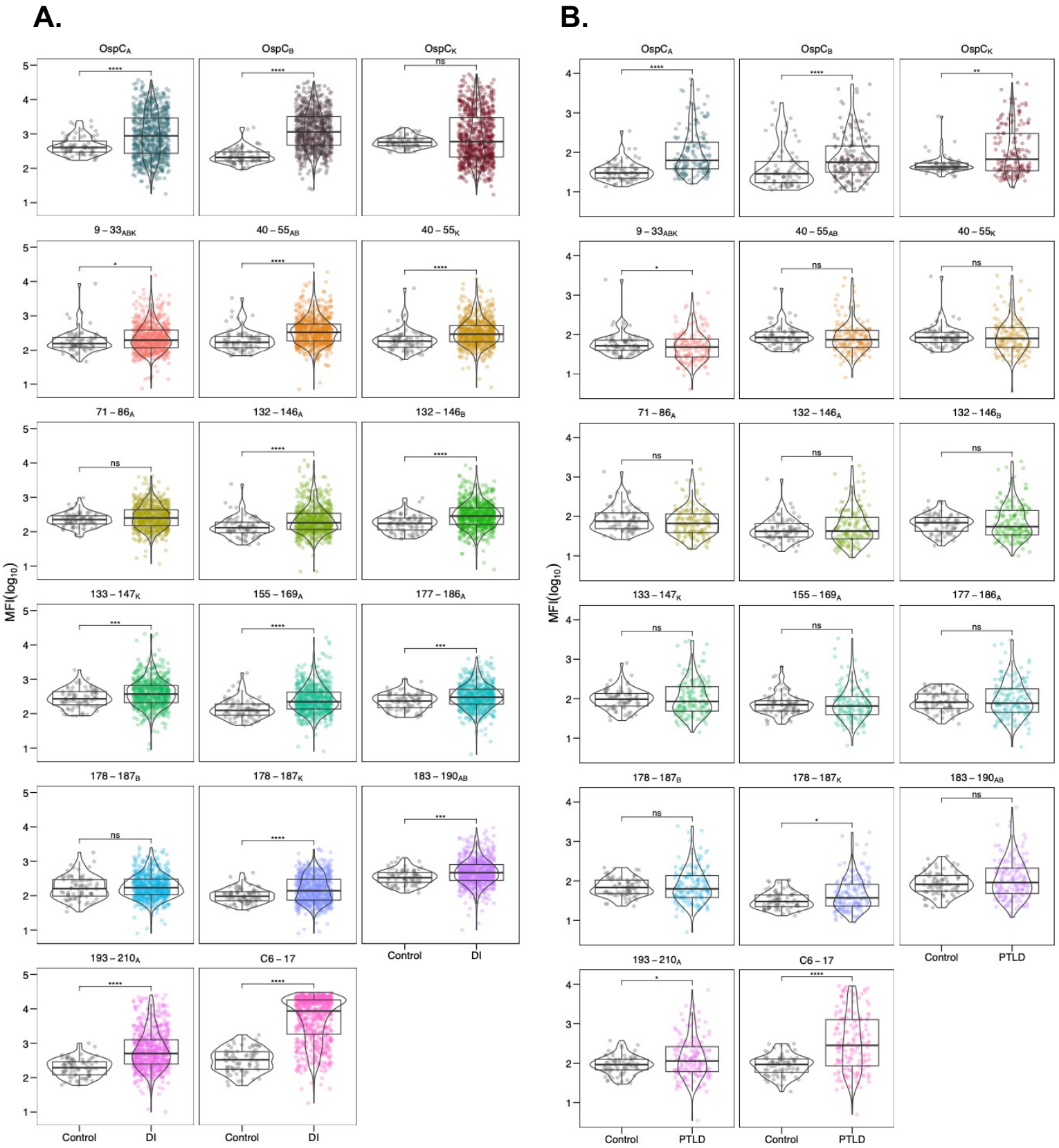
A.
B.
OspC$_A$
OspC$_B$
OspC$_K$
9 – 33$_{ABK}$
40 – 55$_{AB}$
40 – 55$_K$
71 – 86$_A$
132 – 146$_A$
132 – 146$_B$
133 – 147$_K$
155 – 169$_A$
177 – 186$_A$
178 – 187$_B$
178 – 187$_K$
183 – 190$_{AB}$
193 – 210$_A$
C6 – 17
MFI(log$_{10}$)
Control
DI
PTLD

Figure 3

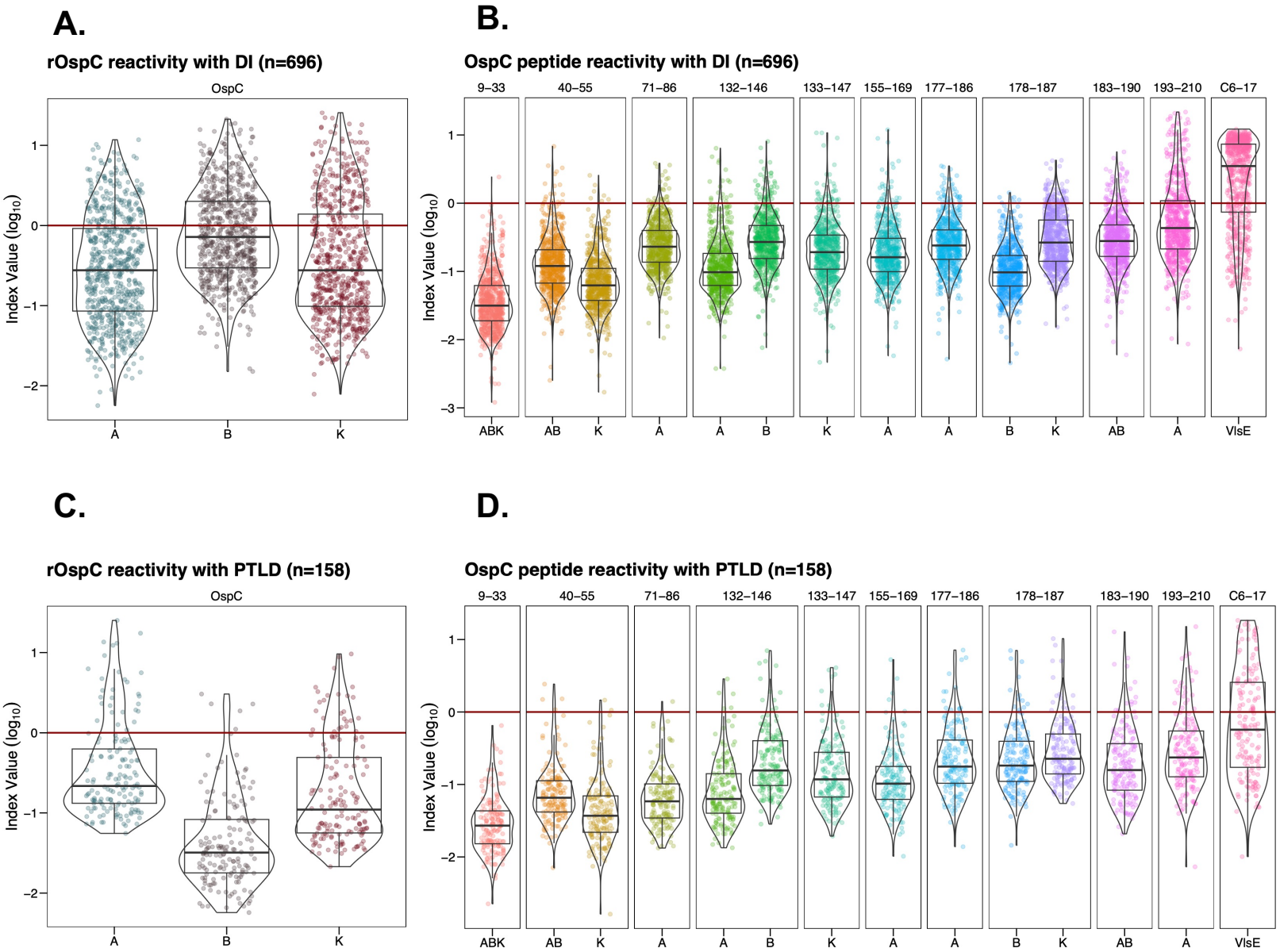
A.
rOspC reactivity with DI (n=696)
OspC
Index Value (log10)
A
B
K
B.
OspC peptide reactivity with DI (n=696)
9–33
40–55
71–86
132–146
133–147
155–169
177–186
178–187
183–190
193–210
C6–17
ABK
AB
K
A
A
B
K
A
A
B
K
AB
A
VlsE
C.
rOspC reactivity with PTLD (n=158)
OspC
D.
OspC peptide reactivity with PTLD (n=158)

Figure 4

A.

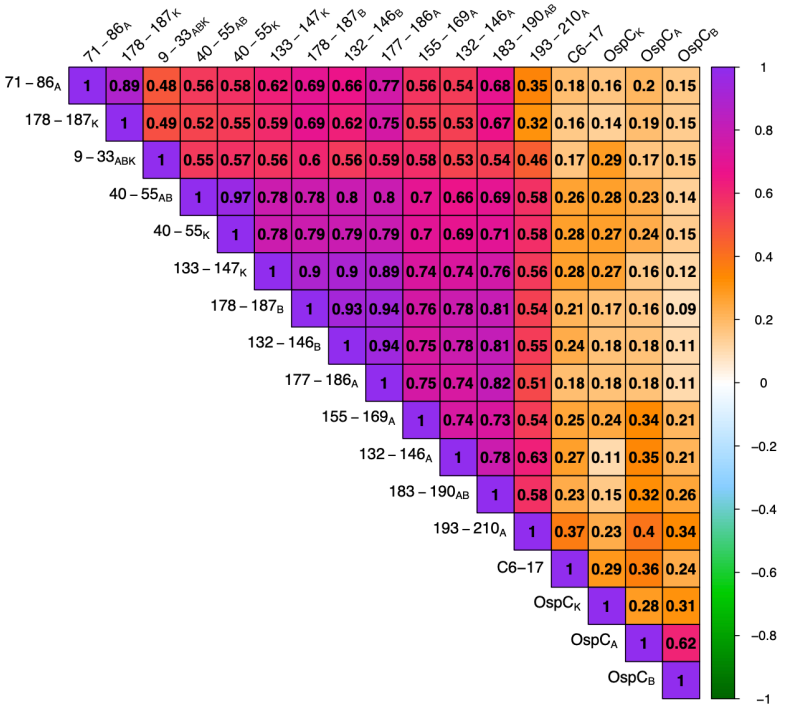
71 – 86A
178 – 187K
9 – 33ABK
40 – 55AB
40 – 55K
133 – 147K
178 – 187B
132 – 146B
177 – 186A
155 – 169A
132 – 146A
183 – 190AB
193 – 210A
C6–17
OspCK
OspCA
OspCB
1 0.89 0.48 0.56 0.58 0.62 0.69 0.66 0.77 0.56 0.54 0.68 0.35 0.18 0.16 0.2 0.15
1 0.49 0.52 0.55 0.59 0.69 0.62 0.75 0.55 0.53 0.67 0.32 0.16 0.14 0.19 0.15
1 0.55 0.57 0.56 0.6 0.56 0.59 0.58 0.53 0.54 0.46 0.17 0.29 0.17 0.15
1 0.97 0.78 0.78 0.8 0.8 0.7 0.66 0.69 0.58 0.26 0.28 0.23 0.14
1 0.78 0.79 0.79 0.79 0.7 0.69 0.71 0.58 0.28 0.27 0.24 0.15
1 0.9 0.9 0.89 0.74 0.74 0.76 0.56 0.28 0.27 0.16 0.12
1 0.93 0.94 0.76 0.78 0.81 0.54 0.21 0.17 0.16 0.09
1 0.94 0.75 0.78 0.81 0.55 0.24 0.18 0.18 0.11
1 0.75 0.74 0.82 0.51 0.18 0.18 0.18 0.11
1 0.74 0.73 0.54 0.25 0.24 0.34 0.21
1 0.78 0.63 0.27 0.11 0.35 0.21
1 0.58 0.23 0.15 0.32 0.26
1 0.37 0.23 0.4 0.34
1 0.29 0.36 0.24
1 0.28 0.31
1 0.62
1
1 0.8 0.6 0.4 0.2 0 −0.2 −0.4 −0.6 −0.8 −1

B.

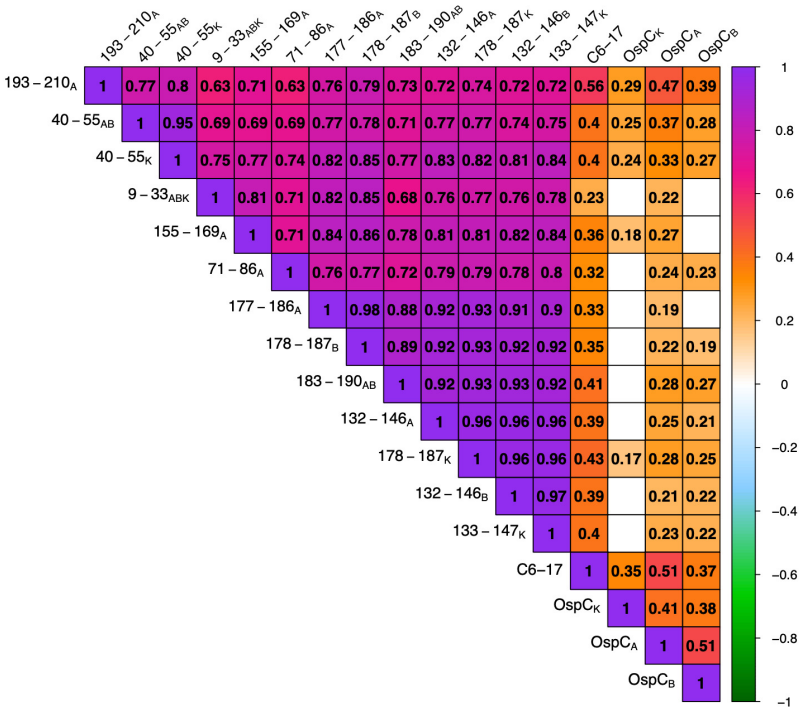
193 – 210A
40 – 55AB
40 – 55K
9 – 33ABK
155 – 169A
71 – 86A
177 – 186A
178 – 187B
183 – 190AB
132 – 146A
178 – 187K
132 – 146B
133 – 147K
C6–17
OspCK
OspCA
OspCB
1 0.77 0.8 0.63 0.71 0.63 0.76 0.79 0.73 0.72 0.74 0.72 0.72 0.56 0.29 0.47 0.39
1 0.95 0.69 0.69 0.69 0.77 0.78 0.71 0.77 0.77 0.74 0.75 0.4 0.25 0.37 0.28
1 0.75 0.77 0.74 0.82 0.85 0.77 0.83 0.82 0.81 0.84 0.4 0.24 0.33 0.27
1 0.81 0.71 0.82 0.85 0.68 0.76 0.77 0.76 0.78 0.23 0.22
1 0.71 0.84 0.86 0.78 0.81 0.81 0.82 0.84 0.36 0.18 0.27
1 0.76 0.77 0.72 0.79 0.79 0.78 0.8 0.32 0.24 0.23
1 0.98 0.88 0.92 0.93 0.91 0.9 0.33 0.19
1 0.89 0.92 0.93 0.92 0.92 0.35 0.22 0.19
1 0.92 0.93 0.93 0.92 0.41 0.28 0.27
1 0.96 0.96 0.96 0.39 0.25 0.21
1 0.96 0.96 0.43 0.17 0.28 0.25
1 0.97 0.39 0.21 0.22
1 0.4 0.23 0.22
1 0.35 0.51 0.37
1 0.41 0.38
1 0.51
1
1 0.8 0.6 0.4 0.2 0 −0.2 −0.4 −0.6 −0.8 −1

Figure 5

A.

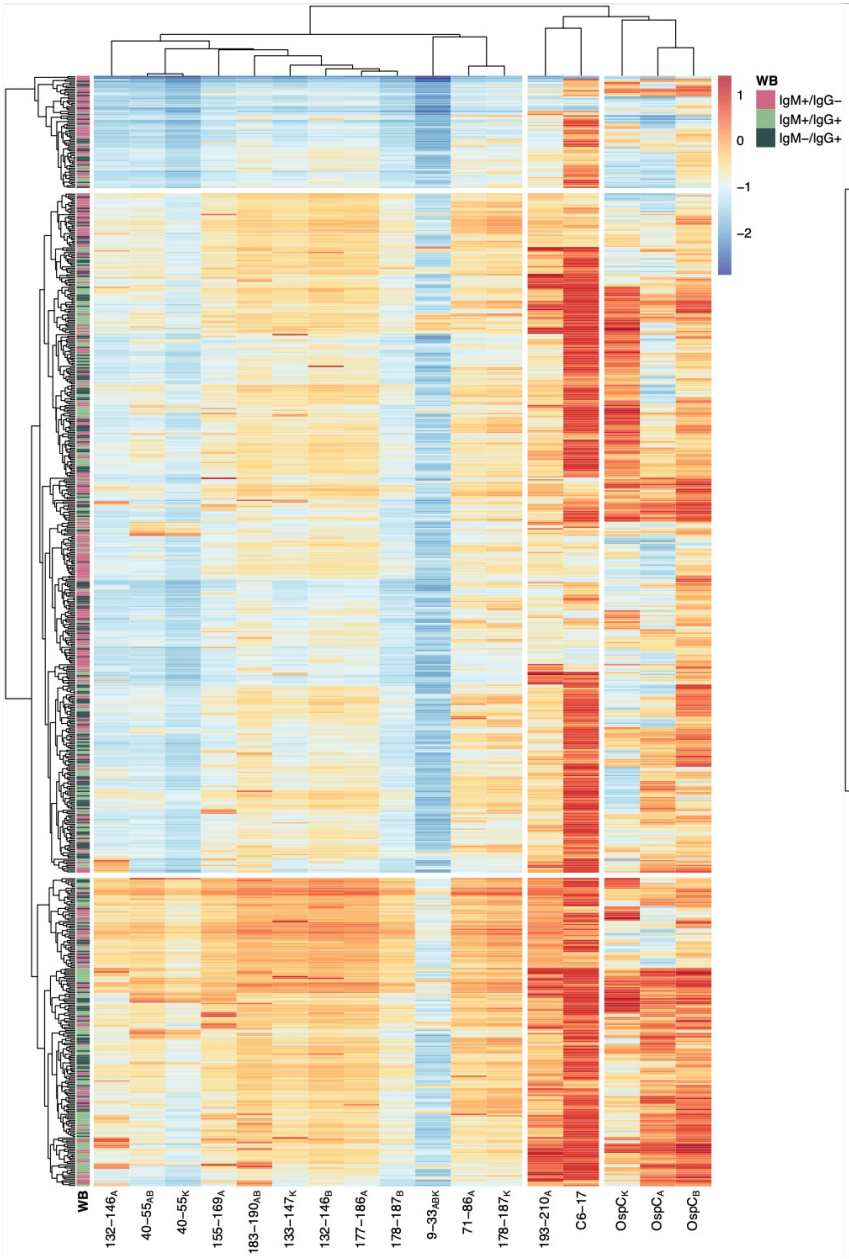
WB
IgM+/IgG−
IgM+/IgG+
IgM−/IgG+
1
0
−1
−2
WB
132–146A
40–55AB
40–55K
155–169A
183–190AB
133–147K
132–146B
177–186A
178–187B
9–33ABK
71–86A
178–187K
193–210A
C6–17
OspCK
OspCA
OspCB

B.

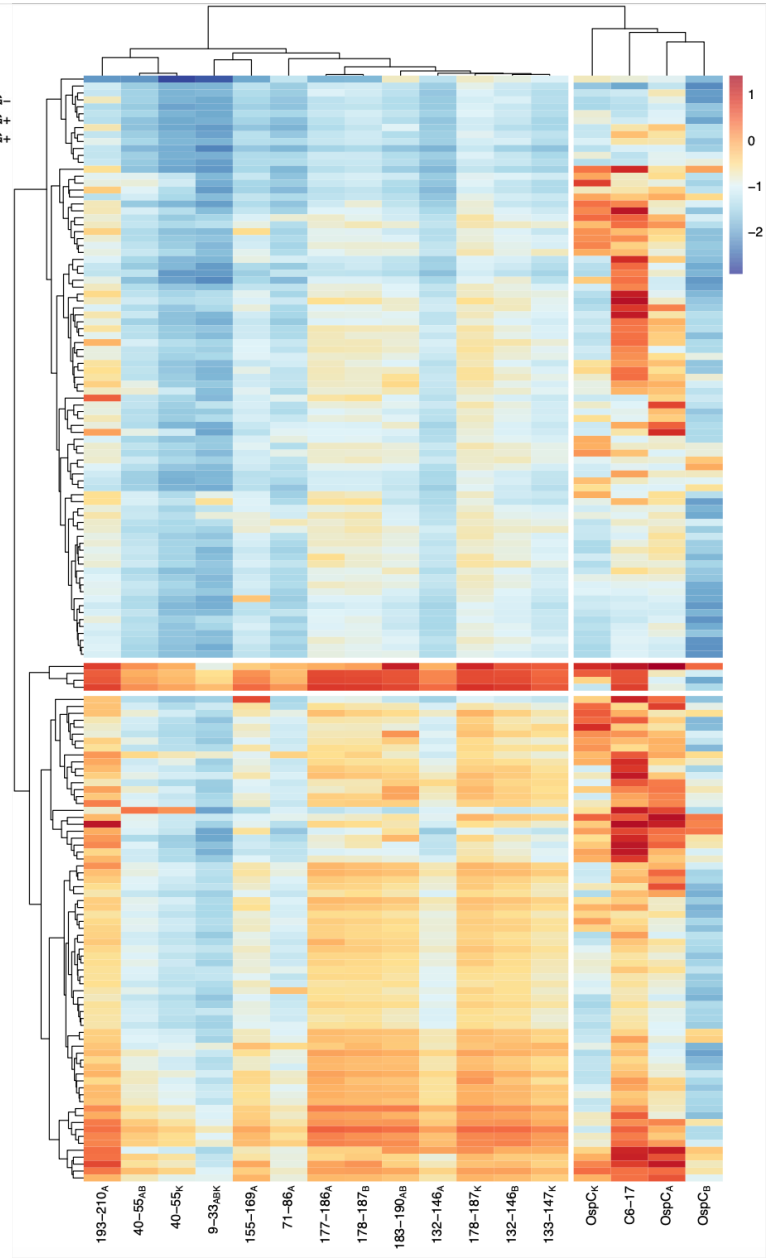
1
0
−1
−2
193–210A
40–55AB
40–55K
9–33ABK
155–169A
71–86A
177–186A
178–187B
183–190AB
132–146A
178–187K
132–146B
133–147K
OspCK
C6–17
OspCA
OspCB

Figure 6

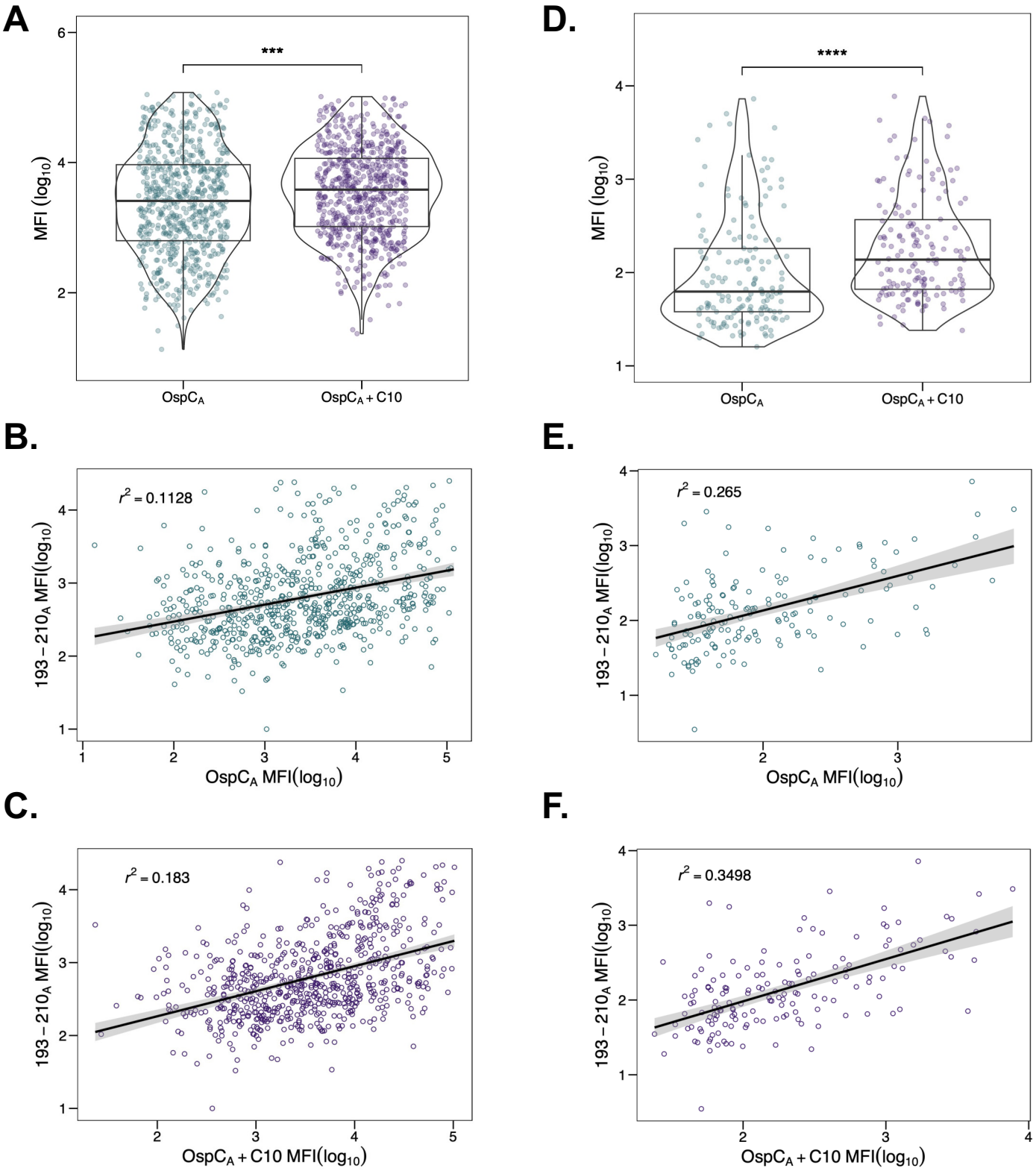
A
***
MFI (log10)
OspCA
OspCA + C10
D.
****
MFI (log10)
OspCA
OspCA + C10
B.
r2 = 0.1128
193 – 210A MFI(log10)
OspCA MFI(log10)
E.
r2 = 0.265
193 – 210A MFI(log10)
OspCA MFI(log10)
C.
r2 = 0.183
193 – 210A MFI(log10)
OspCA + C10 MFI(log10)
F.
r2 = 0.3498
193 – 210A MFI(log10)
OspCA + C10 MFI(log10)